Focused ion beam and field-emission microscopy of metallic filaments in memory devices based on thin films of an ambipolar organic compound consisting of oxadiazole, carbazole, and fluorene units

Christopher Pearson, Leon Bowen, Myung-Won Lee, Alison L. Fisher, Katharine E. Linton, Martin R. Bryce, and Michael C. Petty

Citation: Applied Physics Letters **102**, 213301 (2013); doi: 10.1063/1.4808026
View online: http://dx.doi.org/10.1063/1.4808026
View Table of Contents: http://scitation.aip.org/content/aip/journal/apl/102/21?ver=pdfcov
Published by the AIP Publishing

Focused ion beam and field-emission microscopy of metallic filaments in memory devices based on thin films of an ambipolar organic compound consisting of oxadiazole, carbazole, and fluorene units

Christopher Pearson,[1] Leon Bowen,[2] Myung-Won Lee,[1,a)] Alison L. Fisher,[1] Katharine E. Linton,[3] Martin R. Bryce,[3] and Michael C. Petty[1,b)]
[1]*School of Engineering and Computing Sciences and Centre for Molecular and Nanoscale Electronics, Durham University, Durham DH1 3LE, United Kingdom*
[2]*G. J. Russell Microscopy Facility, Department of Physics, Durham University, Durham DH1 3LE, United Kingdom*
[3]*Department of Chemistry and Centre for Molecular and Nanoscale Electronics, Durham University, Durham DH1 3LE, United Kingdom*

(Received 19 February 2013; accepted 15 May 2013; published online 30 May 2013)

We report on the mechanism of operation of organic thin film resistive memory architectures based on an ambipolar compound consisting of oxadiazole, carbazole, and fluorene units. Cross-sections of the devices have been imaged by electron microscopy both before and after applying a voltage. The micrographs reveal the growth of filaments, with diameters of 50 nm–100 nm, on the metal cathode. We suggest that these are formed by the drift of aluminium ions from the anode and are responsible for the observed switching and negative differential resistance phenomena in the memory devices. © *2013 AIP Publishing LLC*. [http://dx.doi.org/10.1063/1.4808026]

The intense activity in the study of resistive organic memories is motivated by their very simple structure and ability for scaling to small dimensions.[1–5] Such devices can also be stacked in multiple levels, providing 3-D architectures.[6] Despite this impressive progress, there is no agreement on how resistive thin film memories operate. Explanations generally fall into two distinct categories: (i) the injection and storage of charge in the thin film; and (ii) metallic filament formation.[2] In previous work, we have reported on bistable switching phenomena in electroactive organic compounds based on ambipolar compounds, containing both electron and hole transporting groups.[7,8] Our results were inconclusive on the physics of the device operation. Here, we report switching and negative differential resistance (NDR) phenomena in a similar compound and present electron microscopy evidence to support the view that filament formation occurs in the organic layer and is responsible for the switching behavior.

The chemical structure of the compound used in this study, 2-(4-(7-(9*H*-carbazol-9-yl)-9,9-dihexyl-9*H*-fluoren-2-yl)phenyl)-5-(4-*tert*-butylphenyl)-1,3,4-oxadiazole, is shown in Figure 1; the material was synthesized as described previously and has been used in the fabrication of organic light-emitting devices.[9] This compound is a triad molecule: the oxadiazole, carbazole, and fluorene units serve as the electron transport, hole transport, and emitter segments of the molecule. The architecture of the metal/organic compound/metal structures investigated in this work is also depicted in Figure 1. Devices were all prepared in a Class 1000 microelectronics clean room. The substrates were glass microscope slides. These were scrupulously cleaned using the procedure described previously.[8]

The bottom electrodes, consisting of 100 nm thick strips of aluminium 1.5 mm wide and 1.5 mm apart, were deposited by thermal evaporation through a shadow mask at a rate of 0.5 ± 0.1 nm s^{-1} under a vacuum of approximately 5×10^{-6} mbar. Following metallization, the slides were cut into pieces 2 cm long. For some devices, the metallized substrates were spin coated with a 50 nm thick layer of poly(3,4-ethylenedioxythiophene)-poly(styrenesulfonate) from aqueous dispersion (PEDOT-PSS; CLEVIOS P VP AI 4083, Heraeus, Germany). Before coating, the PEDOT-PSS solution was passed through a 0.2 μm syringe filter to remove any residual

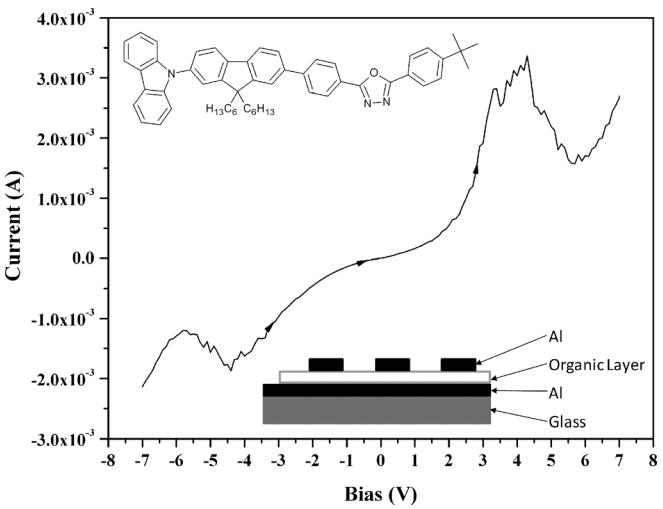

FIG. 1. Current versus voltage scan for a formed memory device based on an Al/organic compound/Al structure. The bias potential refers to that on the bottom Al electrode. The device architecture and the chemical formula for the organic compound are shown in the inset. The top and bottom electrodes consist of sets of aluminium strips, with the top set perpendicular to the bottom set.

[a)]Present address: System LSI Division, Samsung Electronics Co. Ltd., Yongin-City Gyeonggi-do 446-711, Korea.
[b)]Author to whom correspondence should be addressed. Electronic mail: m.c.petty@durham.ac.uk. Tel.: +44 191 334 2419. Fax: +44 191 334 2407.

particulates. Then, 200 μl of the filtered dispersion was applied to the surface of the substrate which was spun at 2500 rpm for 45 s. The PEDOT-PSS coated substrates were annealed at 180 °C for 2 min to remove any residual water.

A solution of the ambipolar compound was prepared by adding 1 ml of Fisher Chemical Trace Analysis Grade chloroform to the solid to give a concentration of 6.70 g l^{-1}. The active organic layer was deposited by spin-coating 150 μl of this solution at 750 rpm for 50 s in a glove-box under a nitrogen atmosphere. To complete the devices, 100 nm thick aluminium strips perpendicular to and having the same dimensions as the bottom electrodes were thermally evaporated on top of the organic layers. The evaporation conditions were the same as those used for the bottom electrodes. The thickness of the organic layer was measured by mechanically removing the film (by abrasion in an area between the metal electrodes) and then imaging the step created using a Digital Instruments NanoMan II AFM in tapping mode. Electrical characterization of the devices was undertaken with the samples in vacuum and using a Keithley 2400 Sourcemeter.

A typical current versus voltage scan of an Al/organic compound/Al device is shown in Figure 1. As reported previously by ourselves and others, a positive voltage had to be applied to the top Al electrode before any switching effects were observed (device "formation"). The current versus voltage characteristics of Fig. 1 (first scan, voltage scanning from a positive potential applied to the top electrode towards a negative potential) exhibit clear regions of NDR in both bias regimes. The devices could also be reversibly switched between high and low conductivity states. The ON state was obtained by applying a voltage close to the current maximum (just before the NDR region) and reducing it rapidly to zero (Write; −4 V in Fig. 1). In contrast, switching from the high conductivity ON state to the OFF sate was accomplished by selecting a voltage near that corresponding to the current minimum in the negative differential resistance region and reducing this rapidly to zero (Erase; −6 V in Fig. 1). The state of the device (ON or OFF) could be determined by measuring the current at a low voltage (Read; −1 V in Fig. 1). The ON and OFF current levels for the devices described in this work were similar to those reported previously, with an ON/OFF current ratio of between 10^2 and 10^3.[7,8]

Focused ion beam (FIB) cross-section cuts through the devices were performed using a FEI Helios Nano Lab 600 Dual Beam system MK2, equipped with a focused Ga liquid metal ion source. Ion beam thinning was carried out at 52° with respect to the electron column for all devices. Initially, a "rough cut" was carried out after first depositing 20 nm of carbon coating followed by a protective platinum layer *in-situ* using a gas injection system. A series of *in-situ* polishing steps were then performed on the exposed cross sections to produce a clean surface with minimal beam damage. High resolution secondary electron imaging was carried out in the same system, with images being captured using low current and kV ultra high resolution immersion lens. An example image is shown in Figure 2. No voltage had previously been applied to this sample. The various layers in the device, and the additional carbon and platinum films, are clearly evident. The average thickness of the spin-coated

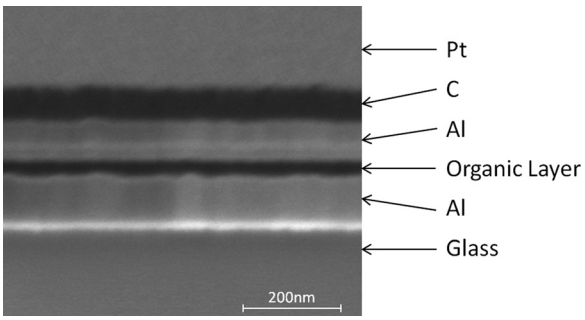

FIG. 2. Electron microscopy image of a cross section of an as-deposited (unformed) Al/organic compound/Al structure.

layer of organic compound is approximately 40 nm. Close inspection of the electron micrograph reveals that this thickness can vary by 20%, due to the relatively uneven surface of the underlying evaporated Al layer.

The same experiment was then undertaken following the application of a positive voltage to the top Al electrode in order to form the memory device. Following this procedure, current versus voltage characteristics similar to those shown in Fig. 1 were obtained by scanning the device between different polarity voltages. Figure 3 shows a series of cross-section electron

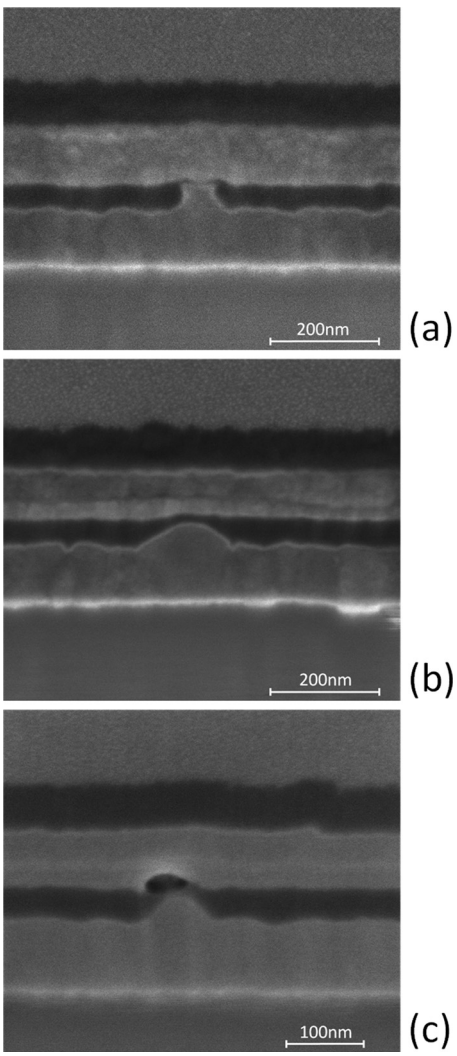

FIG. 3. Electron microscopy images of an Al/organic compound/Al structure following application of a positive voltage (7 V) to the top Al electrode.

micrographs for the formed device structures. What appear to be Al filaments are now evident in the organic film: Fig. 3(a) shows a filament that has completely spanned the organic film; Fig. 3(b) shows a region of the device where the growing filament has not made contact with the top electrode; and Fig. 3(c) seems to depict a situation where the filament has formed between the two metal electrodes and subsequently ruptured in a region adjacent to the top electrode. These filaments are of 50–100 nm in diameter and grow from the bottom aluminium electrode (cathode) and towards the top electrode.

The metallic filamentary model of resistive memories is attractive in that it certainly accounts for the observation of switching and NDR in a wide range of thin film systems and explains the noisy (and somewhat random) nature of the switching events observed by ourselves and others. It also accounts for the observation that the ON-state usually exhibits Ohmic current versus voltage behavior.[8] A model for the growth and thermal rupture of many conducting filaments through the insulating layer, which would account for the switching and NDR, was first suggested by Dearnaley *et al.* in 1970.[10,11] The voltage-controlled or "N-shaped" current versus voltage characteristic (e.g., Fig. 1) results from non-regenerative filament formation, i.e., the resistance of the device is only slightly perturbed by the creation of a filament and the conditions are retained for the development of further filaments. Although, many authors have suggested that filamentary conduction is responsible for switching in organic thin films,[12–16] there have been very few direct microscopy observations of filament formation in memory devices. One exception is the paper of Cho *et al.*[17] which reports on the formation of filamentary paths of silver in Ag/polymer/heavily doped p-type poly Si structures; however, these devices did not appear to exhibit the NDR characteristics noted by ourselves and other researchers.

We suggest that, in the regions where the organic layer is thin, the relatively high electric field results in the injection of Al^{3+} ions into the film. The Al^{3+} ions then drift towards the bottom electrode, where they are reduced to Al metal. Subsequently, aluminium filaments begin to grow on the bottom electrode (which differs from our earlier speculation that aluminium metal diffuses into the organic film from the top electrode[8]). When these have penetrated to the top electrode, the device switches into its high (ON) conductivity state. We consider that the creation of the network of conductive filaments throughout the organic film constitutes the device formation. This process does not occur so easily when the bottom Al electrode is positively biased as the associated aluminium oxide layer will be thicker than that on the underside of the top metal electrode; this asymmetry results from the kinetics of oxide growth on the different electrodes.

The maximum current shown in Fig. 1 (just before the NDR region) is approximately 3 mA (current density approximately $0.13\,A\,cm^{-2}$) at an applied voltage of 4 V. The power dissipation is, therefore, about 12 mW. Assuming that this current is carried mainly through the filamentary regions, it is likely that the resulting power dissipation will lead to filament rupture. However, a filament can subsequently reform by the drift and oxidation of Al^{3+} ions from either electrode (depending on polarity). There will be a dynamic equilibrium between filament formation and destruction, e.g., in the NDR region, the rate of filament rupture will exceed that of filament formation. According to this model, the device formation will depend on redox properties of the organic film and electrodes, and on the ability of the organic layer to transport metal ions, explaining why some metal/thin film/metal devices reported in the literature show no switching, while, in others, "S-shaped" (current-controlled) rather than "N-shaped" (voltage controlled) NDR regions are observed. The chemical nature and morphology of our ambipolar organic compound clearly allows the transport of aluminium ions from the anode and electron injection from the cathode.

Our model can be summarized as follows: device "formation"—filament growth; ON state—filamentary conduction; NDR region—filament destruction exceeds filament formation; OFF state—conduction between broken ends of filaments through the organic film. To test the above conjecture, we have fabricated devices in which a hole transport/electron blocking layer of PEDOT:PSS was interposed between the bottom Al electrode and the spin-coated layer of the ambipolar compound. The resulting current versus voltage characteristics for this structure compared to a "reference" Al/ambipolar organic compound/Al device are shown in Figure 4. These data were obtained for virgin devices and were recorded for increasing positive voltages applied to the top Al electrodes. The reference device shows both switching and NDR regions as the applied voltage is increased. The best fits for the ON and OFF current versus voltage characteristics are of the form $I \propto V^n$, with $n \sim 1.3$, similar to results found previously for a similar ambipolar organic compound.[8] In contrast, the structure containing the electron-blocking layer exhibits neither NDR nor switching phenomena. In this case, the current versus voltage characteristics reveal $\ln(I/V)$ versus $V^{0.5}$, indicative of Poole-Frenkel conductivity. These results are expected from the theory presented above, as electrons from the bottom Al

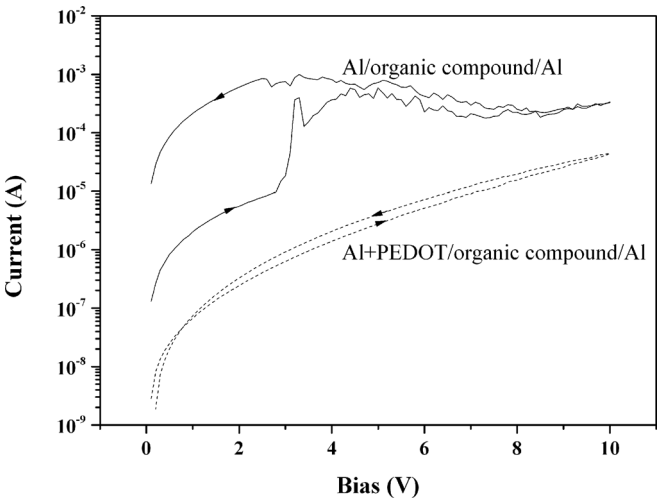

FIG. 4. Current versus voltage characteristics for resistive memory devices showing the effect of incorporating a PEDOT:PSS layer between the bottom Al electrode and the organic film. Full lines correspond to data for Al/organic compound/Al structure, while the broken lines are for the Al + PEDOT/organic compound/Al architecture.

contact will no longer be able to reduce the Al^{3+} ions and the process of filament growth outlined above will not occur.

In summary, we have undertaken an electron microscopy study of switching phenomena in thin film resistive memories based on an ambipolar organic compound. Evidence for filament formation is presented that accounts for the switching and negative differential resistance observed in the devices. It is suggested that the filaments are aluminium, which form on the bottom Al electrode as a result of the drift of Al ions through the films and their subsequent reduction. Clearly, it is now imperative to develop the material design rules in order to optimize the performance of these devices. Filament formation may also have important implications for the operation of organic light-emitting devices, some of which use similar compounds to that used in this work.

The work was supported in part by the U.K. Engineering and Physical Sciences Research Council under Grant No. EP/F017375/1.

[1]J. C. Scott and L. D. Bozano, Adv. Mater. **19**, 1452 (2007).
[2]B. Cho, S. Song, Y. Ji, T.-W. Kim, and T. Lee, Adv. Funct. Mater. **21**, 2806 (2011).
[3]T. W. Kim, Y. Yang, F. Li, and W. L. Kwan, NPG Asia Materials **4**, e18 (2012).
[4]D. B. Strukov and H. Kohlstedt, MRS Bull. **37**, 108 (2012).
[5]T. Lee and Y. Chen, MRS Bull. **37**, 144 (2012).
[6]S. Song, B. Cho, T.-W. Kim, Y. Ji, M. Jo, G. Wanf, M. Choe, Y. H. Kahng, H. Hwang, and T. Lee, Adv. Mater. **22**, 5048 (2010).
[7]C. Pearson, J. H. Ahn, M. F. Mabrook, D. A. Zeze, M. C. Petty, K. T. Kamtekar, C. Wang, M. R. Bryce, P. Dimitrakis, and D. Tsoukalas, Appl. Phys. Lett. **91**, 123506 (2007).
[8]P. Dimitrakis, P. Normand, D. Tsoukalas, C. Pearson, J. H. Ahn, M. F. Mabrook, D. A. Zeze, M. C. Petty, K. T. Kamtekar, C. Wang, M. R. Bryce, and M. Green, J. Appl. Phys. **104**, 044510 (2008).
[9]A. L. Fisher, K. E. Linton, K. T. Kamtekar, C. Pearson, M. R. Bryce, and M. C. Petty, Chem. Mater. **23**, 1640 (2011).
[10]G. Dearnaley, D. V. Morgan, and A. M. Stoneham, J. Non-Cryst. Solids **4**, 593 (1970).
[11]G. Dearnaley, A. M. Stoneham, and D. V. Morgan, Rep. Prog. Phys. **33**, 1129 (1970).
[12]M. Cölle, M. Büchel, and D. M. De Leeuw, Org. Electron. **7**, 305 (2006).
[13]F. Verbakel, S. C. J. Meskers, R. A. J. Janseen, H. L. Gomes, M. Cölle, M. Büchel, and D. M. De Leeuw, Appl. Phys. Lett. **91**, 192103 (2007).
[14]P. Sebastian, F. Lindner, K. Walzer, and K. Leo, J. Appl. Phys. **110**, 084508 (2011).
[15]Z. S. Wang, F. Zeng, J. Yang, C. Chen, Y. C. Yang, and F. Pan, Appl. Phys. Lett. **97**, 253301 (2010).
[16]W.-J. Joo, T.-L. Choi, J. Lee, S. K. Lee, M.-S. Jung, N. Kim, and J. M. Kim, J. Phys. Chem. B **110**, 23812 (2006).
[17]B. Cho, J.-M. Jun, S. Song, Y. Ji, D.-Y. Kim, and T. Lee, Adv. Funct. Mater. **21**, 3976 (2011).